Materials Science and Engineering A 386 (2004) 284–290

MATERIALS SCIENCE & ENGINEERING A

www.elsevier.com/locate/msea

Microstructure and microhardness of SiC nanoparticles reinforced magnesium composites fabricated by ultrasonic method

Jie Lan[a], Yong Yang[b], Xiaochun Li[b,*]

[a] *Materials Science Program, University of Wisconsin-Madison, WI 53705, USA*
[b] *Department of Mechanical Engineering, University of Wisconsin-Madison, WI 53705, USA*

Received 7 June 2004

Abstract

The use of ultrasonic non-linear effects to disperse nano-sized ceramic particles in molten metal has been studied and nano-sized SiC particle reinforced AZ91D magnesium composites were fabricated. The microstructure of the composites was investigated by high-resolution scanning electron microscopy (SEM), X-ray photo spectroscopy (XPS), and high-resolution X-ray diffractometer (XRD) techniques. Experimental results show a nearly uniform distribution and good dispersion of the SiC nanoparticles within the magnesium matrix, although some of small agglomerates (less than 300 nm) were found in matrix. Detailed study reveals that the SiC nanoparticles were partially oxidized. The microhardness of composites have been improved significantly compared to that of pure AZ91D. The interaction between SiC nanoparticles and the matrix was investigated. The interaction between ultrasonic waves and nanoparticles was also discussed. The ultrasonic fabrication methodology is striking to rapidly produce a wide range of nano-sized particles reinforced metal matrix composites.

Keywords: Metal matrix nanocomposite; Magnesium alloy; SiC nanoparticle

1. Introduction

Metal matrix composites (MMC) are attractive in various applications because of their improved properties. Significant efforts have been taken to develop magnesium matrix composites in recent years due to their low density, high strength, superior creep resistance, high damping capacity, and good dimensional stability [1–21]. Magnesium matrix composites are excellent candidates as structural materials, and have great potential in automotive and aerospace applications. Discontinuous micro-scale reinforcements such as short fibers [1,2], particles [3–5], or whiskers [5,6], have been used to produce magnesium MMCs.

The strengthening mechanism for MMCs with fine particles has been theoretically studied [22,23]. It is believed that the properties of metal matrix composites with embedded nano-sized ceramic particles (less than 100 nm) would be enhanced considerably even with a very low volume fraction of these nanoparticles. The potential advantages of these metal matrix nanocomposites (MMNCs) have generated excitement in both academia and industry. The need for cast structural components of high-performance magnesium alloy composites is expected to increase as automotive industries are forced to improve the fuel efficiency of their products.

Conventional fabrication methods, such as mechanical stir casting [4–12], powder metallurgy [13,14], and squeeze casting [15–18] have been applied to produce discontinuously micro particles reinforced magnesium MMCs. Among these methods, stir casting is an easily adaptable and cost-effective method. This technique is also capable of the near-net-shape formation of the composites into complex shapes by conventional foundry processes. However, it is extremely difficult for the mechanical stirring method to distribute and disperse nano-scale particles uniformly in metal melts due to their large surface-to-volume ratio and their low wettability in metal melts, which easily induce agglomeration and clustering. In this study, high-intensity ultrasonic waves with

* Corresponding author. Tel.: +1 608 262 6142; fax: +1 608 265 2316.
E-mail address: xcli@engr.wisc.edu (X. Li).

0921-5093/$ – see front matter © 2004 Elsevier B.V. All rights reserved.
doi:10.1016/j.msea.2004.07.024

Table 1
Chemical composition of AZ91D magnesium alloy

AZ91D	Mass percentage
Al	9.30
Zn	0.71
Mn	0.21
Si	<0.10
Cu	<0.030
Ni	<0.005
Fe	<0.002
Mg	Balance

Table 2
Chemical composition of nano-sized SiC particle

β-SiC	Mass percentage
SiC	>=95%
[O]	1–1.5%
C	1–2%
Average diameter	30 nm
Specific surface area	>109.0 M^2/g
Synthesis technique	Laser

strong micro scale transient cavitations and acoustic streaming [29,30] were successfully introduced to distribute and disperse nanoparticles into magnesium alloy melts, thus making the production of cast high-performance nano-sized particles reinforced magnesium matrix composite promising.

In this paper, SiCp/AZ91D composites were fabricated by casting with the help of high-intensity ultrasonic wave technique. The microstructure and microhardness of nano-sized SiC particles reinforced magnesium composites are investigated.

2. Experimental procedures

AZ91D magnesium alloy was selected as the matrix of the magnesium composite. Its chemical composition is listed in Table 1. The melting temperature range of this magnesium alloy is 468–596 °C. The reinforcements were silicon carbide nanoparticles with a normalized average diameter of 30 nm. Its chemical composition is shown in Table 2. Magnesium

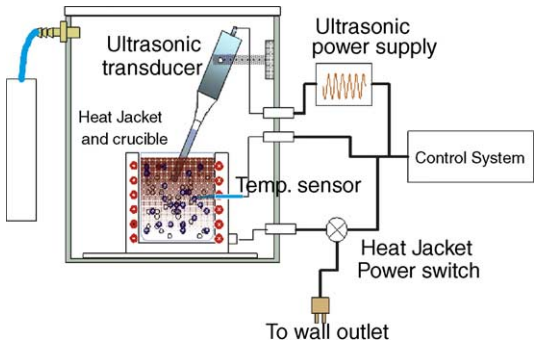

Fig. 1. Schematic of experimental setup.

composites with 2.0 wt.% and 5.0 wt.% nano-sized SiC were prepared.

High-intensity ultrasonic wave was used for processing AZ91D alloy melts. As shown in Fig. 1, the experimental setup consists of processing units and controlling units. A heating unit was used to melt AZ91D in a small graphite crucible of 2″ diameter × 2″ height. A titanium waveguide, which was coupled with a 20 KHz 600 W ultrasonic transducer (Misonix), was dipped into the melt to process the melts. The magnesium melt pool was protected by CO_2/SF_6 (volume ratio 99:1) mixed gas. Nano-sized SiC was added to the crucible from the top surface of the melts. One temperature probe was used to monitor the processing temperature.

The ultrasonic processing temperature was controlled at 620 °C. An ultrasonic power of 80 W from the transducer was found to generate adequate non-linear effects [29,30] inside the crucible. A graphite permanent mold with protection of the mixed gas was used to obtain as-cast bulk nanocomposites. With nano-sized SiC particles in the melts, the viscosity of melts became higher. Thus, after efficient ultrasonic processing, a higher casting temperature of 700 °C was used to ensure a satisfactory flowability inside the mold. It should be noted no ultrasonic wave used during the casting process.

For microstructural study, samples of as-cast bulk magnesium composites were cut, mounted, mechanically ground,

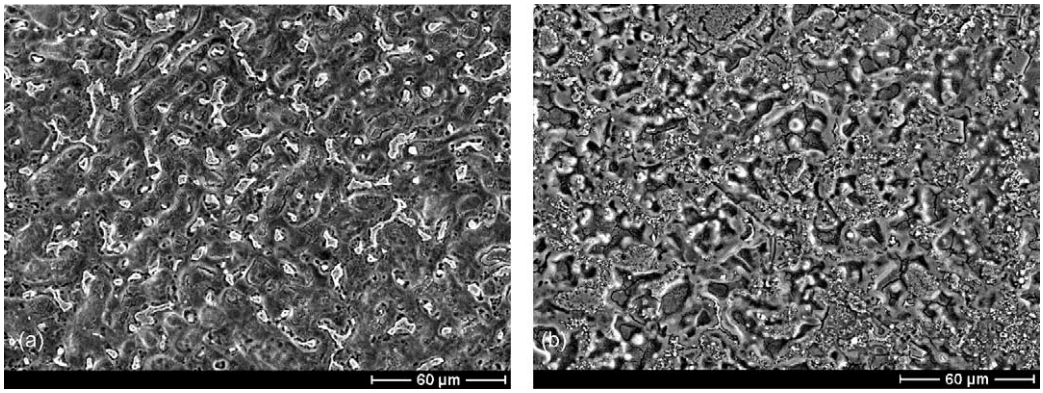

Fig. 2. The microstructure of (a) AZ91D and (b) AZ91D/5SiC.

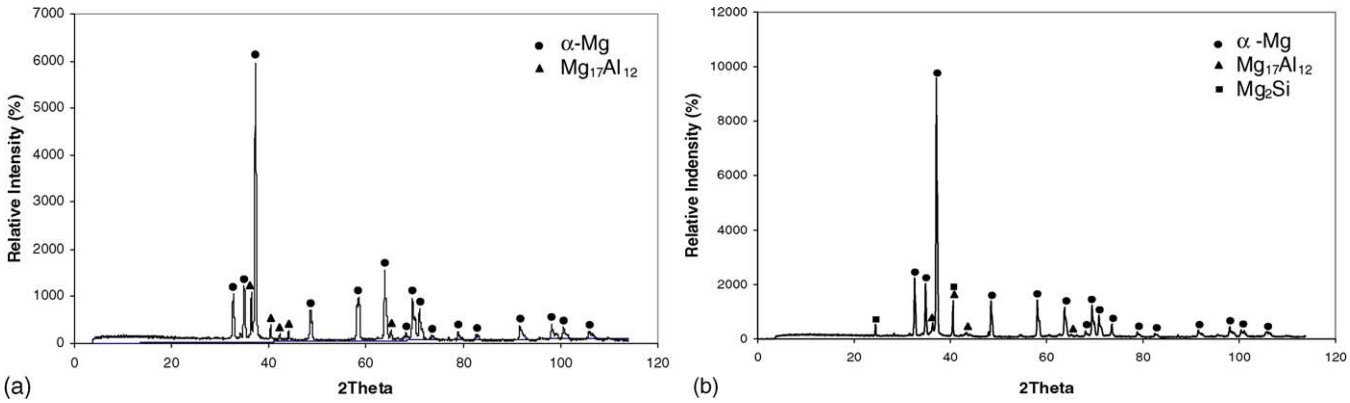

Fig. 3. X-ray diffraction patterns of (a) AZ91D and (b) AZ91D/5SiC.

and finally polished down to 0.05 μm. Specimens for SEM observation were etched with a 2.0 vol.% solution of nitric acid in ethanol for 5 s at room temperature, and then sputtered with Au for better conductivity. The distribution of the nanoparticles and individual elements in the composite phases were investigated with a scanning electron microscopy (*LEO 1530* SEM), equipped with an EDS detector. Inel X-ray detector was used to determine the phases in materials (40 KV, 30 mA).

The X-ray photoelectron spectroscopy (XPS) was introduced to analyze the chemical status of SiC in Mg matrix. Usually X-ray diffraction (XRD) has been used for phase analysis but is of limited value in this study, since only a small volume fraction of SiC nanoparticles were used in this study. The XPS technique uses low energy monochromatic X-ray beams to emit photoelectrons. Elements exhibit binding energy peaks whose relative position depends on the electronegativity of their surrounding atomic neighbors. In the

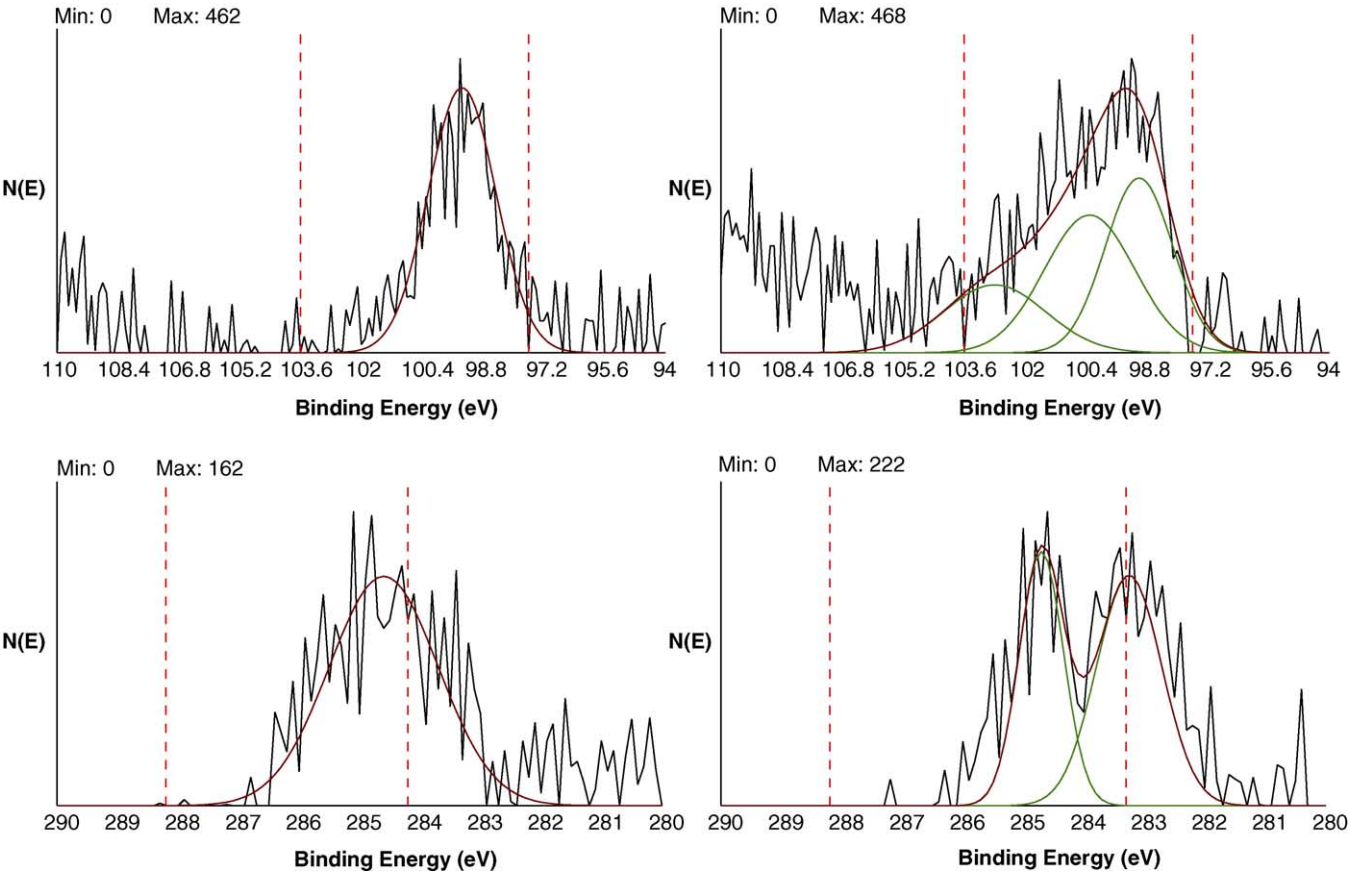

Fig. 4. XPS spectra. (a) Si 2p for AZ91D; (b) Si 2p for AZ91D/5SiC; (c) C 1s for AZ91D; (d) C 1s for AZ91D/5SiC.

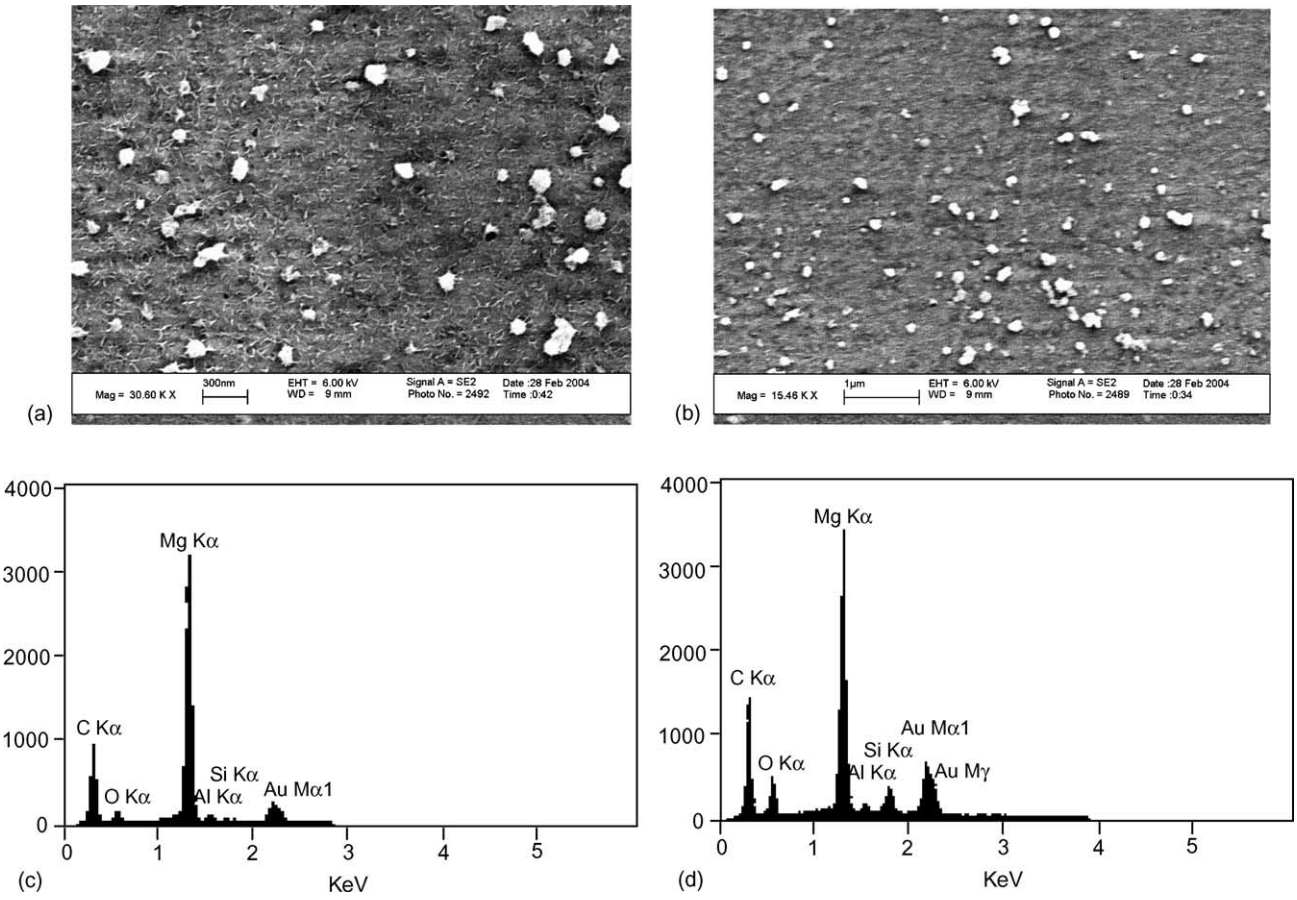

Fig. 5. Distribution and dispersion of SiC nanoparticles in AZ91D/5SiC and spectrum of EDS. (a) SiC in AZ91D; (b) SiC in AZ91D/5SiC under higher magnification; (c) EDS spectrum for matrix near nanoparticles; (d) EDS spectrum for SiC.

case of a phase mixture where more than one bonding state exists, a particular element is expected to have various binding energies, caused by a different coordination/neighbor.

For XPS analysis, samples were ultrasonically cleaned in methanol acetone and ethanol and allowed to air dry, then mounted on an aluminum block fixed to the end of a rotatable probe. The samples were then gradually degassed in the sample introduction chamber and placed into the high vacuum chamber of the XPS spectrometer (*PHI 5400 ESCA/XPS*) for examination. All XPS experiments were conducted at ambient temperature. Following an initial set of XPS survey as a baseline; each sample was sputter cleaned using 25 KV Ar+ for XPS survey followed by C1s high-resolution spectra being taken in 15-min intervals. This was done until the carbon signature was reduced to approximately consistent spectra. The specimen was irradiated with monochromated Mg Ka radiation (Mg anode under KeV and MA). A broad energy scan of all samples was firstly obtained at 2 eV/s in the range of 0–1000 eV. The strong photoelectron lines were then scanned over a 35.77 eV range at a rate of 0.1 eV/s. the signal curves were fitted by peak addition using Gaussian-Lorenzian peak approximations and Shirley background reduction.

The microhardness test was conducted with a Buehler microhardness tester (load 500 gf, load time 30 s, T = 25).

3. Results

3.1. Solidification microstructure

Fig. 2 shows the microstructure of pure AZ91D and AZ91D with 5.0 wt.% SiC (hereafter AZ91D/5SiC). The microstructure of AZ91D alloy consists of a distribution of α-Mg grains together with intergranular β-$Mg_{17}Al_{12}$. The halo surrounding the intermetallic phases is due to a difference in etching characteristics between the α-Mg (higher in Al content), which formed during the last stages of the solidification sequence, and the bulk of the α-Mg grains. The eutectic is divorced and therefore the β-$Mg_{17}Al_{12}$ is shown.

Microstructure of AZ91/5SiC also shows a similar segregation of aluminum in the magnesium matrix, manifesting itself by an increased Al concentration in regions close to the secondary phases. Moreover, EDS analyses show Si-rich precipitates in the AZ91/5SiC. According to XRD patterns of (Fig. 3), these precipitates in AZ91D/5SiC were identified as Mg_2Si, an intermetallic phase of the Mg–Si system. However, it was difficult to verify the SiC phase from the XRD results because of the low percentage and small size of SiC in the matrix.

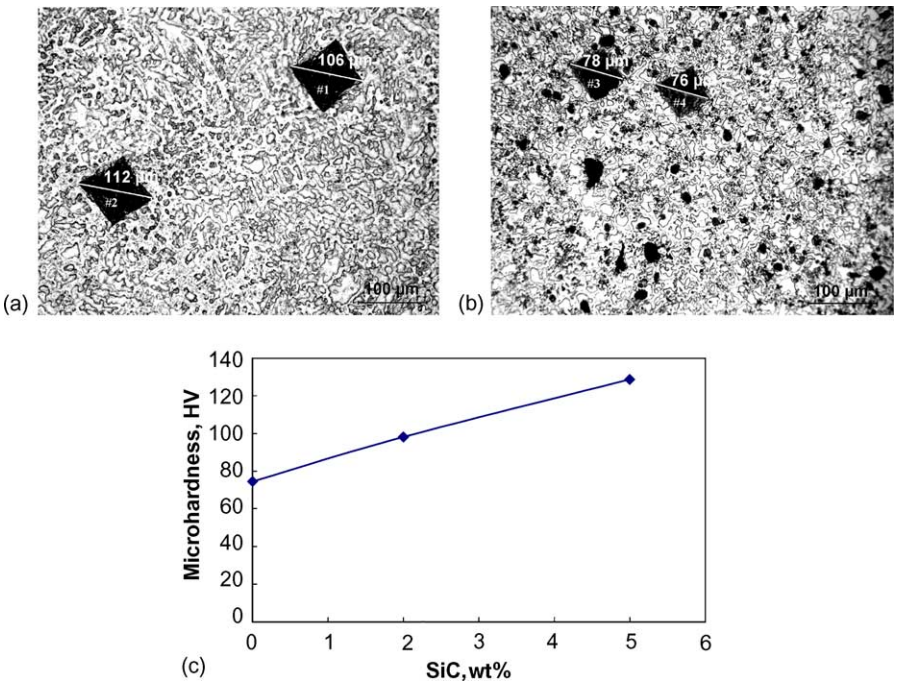

Fig. 6. Microhardness results. (a) Indentations in AZ91D; (b) indentations in AZ91D/5SiC; (c) microhardness comparison of AZ91D, AZ91D/2SiC, and AZ91D/5SiC (each value is the average from at least five tests).

To investigate the interaction between SiC and Mg melts, XPS spectra from the samples were collected. The XPS results of AZ91D and AZ91D/5SiC are shown in Fig. 4. The Si2p of AZ91D consisted of one peak at 99.35 eV that is identified as Si. However, the Si2p of AZ91D/5SiC spectra consisted of three peaks at 99 eV, 100.3 eV, and 102.8 eV. These were identified as those due to Si, SiC, SiO_2, respectively [24–28]. C 1s spectra of AZ91D show the one peak 284.5 eV that is primarily hydrocarbon, a common contaminant. C 1s spectra of AZ91D/5SiC consisted of two peaks: 283.5 eV and 284.5 eV. One of the peaks (284.5 eV) is attributed to contaminant carbon and the other one (283.5 eV) at the lower binding energy side is due to SiC. This result is consistent with that obtained for Si2p in Fig. 4(b). XPS analysis indicates the presence of SiC in AZ91D/5SiC and moreover SiC are partly oxidized.

Fig. 5 shows that the morphology and distribution of SiC nanoparticles in the AZ91D matrix. It can be seen that nanoparticles are well distributed and dispersed, although there are some SiC agglomerates ~100–300 nm in the matrix. In order to determine the chemical composition of the nanoparticles in the magnesium matrix, energy dispersion spectrum (EDS) was used. Because the detection zone of EDS beam is bigger than the average size of SiC, the EDS peaks for SiC nanoparicles (Fig. 5c) will inevitably include compositional information of Mg matrix near particles. However, through subtracting the compositional information of matrix (Fig. 5d), it is evident that Si, C, and O peaks correspond only to composition of nanoparticles. It suggested that the SiC particles are partly oxidized.

3.2. Microhardness test

The micro-scale indentations in AZ91D and AZ91D were shown in Fig. 6. Indentations #1 and #2 in Fig. 6a indicate the hardness of AZ91D including α-Mg and $Mg_{12}Al_{17}$. Indentation #3 in Fig. 6b indicates the hardness of α-Mg and $Mg_{12}Al_{17}$ in AZ91D/5SiC while indentation #4 indicates the hardness of Mg_2Si. From the hardness results, it is shown that the length of hexagonal of indentation in AZ91D/5SiC was obviously shorter than that in AZ91D, indicating that the hardness of AZ91D/5SiC is greater than AZ91D. Additionally, the hardness of Mg_2Si was similar to the matrix of AZ91D/5SiC. SiC nanoparticle distributed in the Mg matrix is attributed to the improved hardness of the nanocomposites.

As shown in Fig. 6c, the hardness of the magnesium composites increased with the increasing percentages of SiC in AZ91D. For AZ91D/5SiC, the average hardness increased by approximately 75% compared to AZ91D.

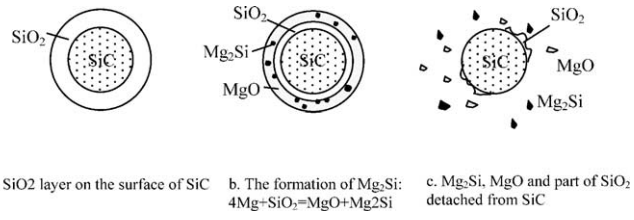

Fig. 7. The schematic of Mg_2Si formation in AZ91/5SiC.

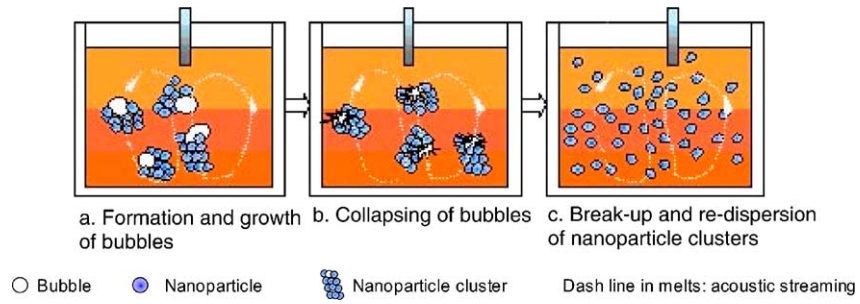

Fig. 8. Schematic of the cavitation and streaming effects for nanoparticle dispersion and wetting in metal melts.

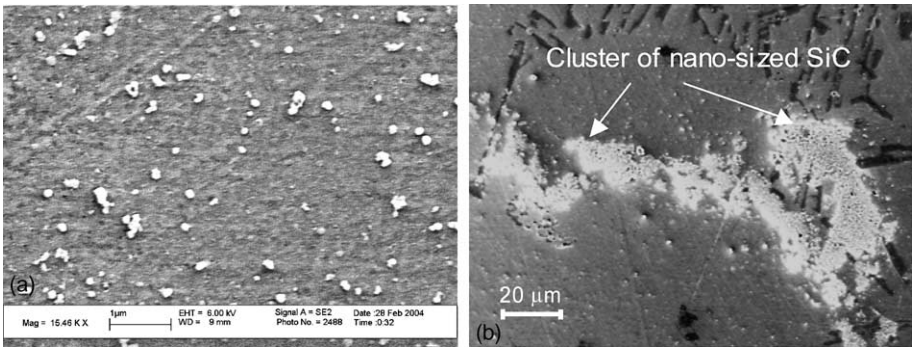

Fig. 9. SiC clusters in AZ91D. (a) Ultrasonic stirring method and (b) traditionally mechanical stirring.

4. Discussion

4.1. Mg_2Si in AZ91D/5SiC

Mg_2Si compound is found in AZ91D/5SiC, but not in AZ91D. It is believed that during the melting and ultrasonic processing, free Si or SiO_2 from the SiC particles together with Mg forms Mg_2Si at the matrix/SiC interface. Because the MgO is loosely on the surface of SiC, the Mg_2Si and MgO phases on the surface of SiC will be detached from SiC under intensive ultrasonic cavitation. From the analysis of EDS for SiC nanoparticles, it indicated that there were no Mg_2Si and MgO exist at the matrix/SiC interface (Fig. 7).

4.2. The interaction between high-intensity ultrasonic waves and nano-sized particle clusters in magnesium melts

High-intensity ultrasonic waves are especially useful in that they generate some important non-linear effects in liquids, namely transient cavitation and acoustic streaming [29,30], which are mostly responsible for benefits including refining microstructures, degassing of liquid metals for reduced porosity, and dispersive effects for homogenizing [31–33]. Acoustic streaming, a liquid flow due to acoustic pressure gradient, is very effective for stirring [34]. Acoustic cavitation involves the formation, growth, pulsating, and collapsing of tiny bubbles in liquid under cyclic high-intensity ultrasonic waves (thousands of micro bubbles will be formed, expanding during the negative pressure cycle and collapsing during the positive pressure cycle). By the end of one cavitation cycle, the tiny bubbles implosively collapse (in less than 10^{-6} s), producing transient (in the order of microseconds) micro "hot spots" that can reach temperatures of about 5000 °C, pressures of about 1000 atm, and heating and cooling rates above 10^{10} K/S [35]. Transient cavitations could produce an implosive impact, which could be strong enough to break up the clustered fine particles to disperse them more uniformly in liquids. The strong impact coupling with local transient high temperatures could enhance the wettability between metal melts and particles significantly (Fig. 8).

It has been demonstrated in Fig. 5 that SiC nanoparticles can be nearly uniformly distributed in the AZ91D matrix by high-intensity ultrasonic waves. Although some small agglomerates in AZ91D/5SiC still existed in the matrix, the agglomerates have been greatly improved when compared with the severe agglomerates in composites fabricated by traditionally mechanical stirring, as shown in Fig. 9.

5. Conclusions

Nano-sized SiC particles reinforced magnesium composites were fabricated by casting with the help of high-intensity

ultrasonic cavitation technique. From the study of microstructural characterization and hardness determination, the results suggest:

High-intensity ultrasonic waves are capable of distributing and dispersing nanoparticles in Mg matrix with non-linear effects in liquids, especially transient cavitation. From the high-resolution SEM observation, SiC nanoparticles are almost uniformly distributed in the matrix, although some small clusters (less than 300 nm) still exist in matrix. EDS analysis indicates that the SiC nanoparticels are partly oxidized.

Compared to pure cast AZ91D, cast AZ91D/5SiC yields Mg_2Si compounds. The Mg_2Si compound in the composites might be resulted from chemical reactions taking place during the ultrasonic processing of composites. Si could be introduced into the magnesium matrix by reactions between Mg and the SiO_2 layer that covers the surfaces of SiC nanoparticles. The XPS analysis also indicates the existence of SiO2.

The microhardness of nanoparticle reinforced magnesium composites improved with the increasing fraction of SiC nanoparticles. The microharness of AZ91D/5SiC increased by 75% compared to that of AZ91D.

References

[1] K.U. Kainer, B.L. Mordike, F. Hehmann (Eds.), Magnesium Alloys and Their Applications, DGM Informationsgesellschaft, Oberursel, Germany, 1993, p. 415.
[2] T. Wada, T. Shinkawa, S. Kamado, Y. Kojima, J. Jpn. Inst. Light Met. 45 (1995) 510.
[3] D.M. Lee, B.K. Suh, B.G. Kim, J.S. Lee, C.H. Lee, Mater. Sci. Technol. 13 (1997) 590.
[4] A. Luo, Metall. Mater. Trans. 26A (1995) 2445.
[5] V. Laurent, P. Jarry, G. Regazzoni, D. Apelian, J. Mater. Sci. 27 (1992) 447.
[6] A. Martin, J. Llorca, Mater. Sci. Eng. A201 (1995) 77.
[7] R.A. Saravanan, M.K. Surappa, Mater. Sci. Eng. A276 (2000) 108.
[8] S.C. Sharma, B. Anand, M. Krishna, Wear 241 (2000) 33.
[9] A. Bochenek, K.N. Braszczynska, Mater. Sci. Eng. A290 (2000) 122.
[10] Y. Cai, M.J. Tan, G.J. Shen, H.Q. Su, Mater. Sci. Eng. A282 (2000) 232.
[11] H. Hu, Scripta Mater. 39 (1998) 1015.
[12] T. Imai, S.W. Lim, D. Jiang, Y. Nishida, T. Imura, Mater. Sci. Forum 304 (1999) 315.
[13] H. Ferkel, B.L. Mordike, Mater. Sci. Eng. A298 (2001) 193.
[14] B.W. Chua, L. Lu, M.O. Lai, Compos. Struct. 47 (1999) 595.
[15] C. Mayencourt, R. Schaller, Mater. Sci. Eng. A325 (2002) 286.
[16] M. Yoshida, S. Takeuchi, J. Pan, G. Sasaki, N. Fuyama, T. Fujii, H. Fukunaga, Adv. Compos. Mater. 8 (1999) 258.
[17] L. Hu, E. Wang, Mater. Sci. Eng. A278 (2000) 267.
[18] M.Y. Zheng, K. Wu, C.K. Yao, Mater. Sci. Eng. A318 (2001) 50.
[19] S. Chang, H. Tezuka, A. Kamio, Mater. Trans. 38 (1997) 18.
[20] S. Ryu, J. Kaneko, M. Sugamata, J. Jpn. Inst. Met. 61 (1997) 1160.
[21] V. Laurent, P. Jarry, G. Regazzoni, D. Apelian, J. Mater. Sci. 27 (1992) 447.
[22] R.J. Arsenault, Mater. Sci. Eng. 64 (1984) 171.
[23] N. Ramakrishnan, Acta Mater. 44 (1996) 69.
[24] K.R. Karasek, S.A. Bradley, J.T. Donner, H.C. Yeh, J.L. Schienle, H.T. Fang, J. Am. Ceram. Soc. 72 (1989) 1907.
[25] Y. Mizokawa, K.M. Geib, C.W. Wilmsen, J. Vac. Sci. Technol. A4 (1986) 1696.
[26] V.M. Bermudez, J. Appl. Phys. 63 (1998) 4951.
[27] Y. Mizokawa, S. Nakanishi, O. Komoda, S. Miyase, H.S. Diang, C.H. Wang, N. Li, C. Jiang, J. Appl. Phys. 67 (1990) 264.
[28] J.F. Moulder, W.F. Stickle, PlE. Sobol, K.D. Bomben, Handbook of X-ray Photoelectron Spectroscopy, Physical Electronics Inc., Minnesota, 1995.
[29] K.S. Suslick (Ed.), Ultrasound: its Chemical, Physical, and Biological Effects, VCH, New York, 1988.
[30] O. Abramov, Ultrasound in Liquid and Solid Metals, CRC Press, Boca Raton, FL, 1994.
[31] J.P. Gabathuler, et al., Processing of Semi-Solid Alloys and Composites, Cambridge, MA, 1992.
[32] D. Goel, D. Shunkla, P. Pandey, Trans. Indian Inst. Met. 3 (1980) 196.
[33] C. Vivès, JOM 50 (1998) 50.
[34] L. Ma, F. Chen, G. Shu, J. Mater. Sci. Lett. 14 (1995) 649.
[35] K.S. Suslick, Y. Didenko, M.M. Fang, T. Hyeon, K.J. Kolbeck, W.B. McNamara, M.M. Midleleni, M. Wong, Phil. Tans. R. Soc. Lond. A 357 (1999) 335.